Hindawi
Advances in Civil Engineering
Volume 2023, Article ID 6610224, 9 pages
https://doi.org/10.1155/2023/6610224

Research Article

Research on the Estimation Model of Energy Consumption Capacity for Reinforced Concrete Components with Axial Force

Yukui Wang[1], **Shijun Yan**[2], **Dan Zhang**[1,3] and **Zhangqi Hu**[4]

[1]*Hunan Engineering Research Center of Development and Application of Ceramsite Concrete Technology, Hunan City University, Yiyang 413099, China*
[2]*College of Mechanical and Electrical Engineering, Hunan City University, Yiyang 413099, China*
[3]*Key Laboratory of Green Building and Intelligent Construction in Higher Educational Institutions of Hunan Province, Hunan City University, Yiyang 413000, China*
[4]*College of Civil Engineering, Hunan City University, Yiyang 413099, China*

Correspondence should be addressed to Yukui Wang; 1219464373@qq.com

Received 10 June 2023; Revised 2 December 2023; Accepted 6 December 2023; Published 19 December 2023

Academic Editor: Tariq Umar

The research group utilized the estimation model of energy consumption capacity for reinforced concrete components without axial force to assess the energy consumption capacity of 92-reinforced concrete components from the PEER database, which were subjected to axial force and bending. The study also examined the impact of design parameters, including longitudinal reinforcement ratio, transverse reinforcement ratio, axial compression ratio, and shear-span ratio, on the estimation results. The research findings revealed that when applying the estimation model of energy consumption capacity for reinforced concrete components without axial force to calculate the energy consumption capacity of reinforced concrete components with axial force, there was a significant deviation rate in the estimation of cumulative energy consumption. The relationship between the deviation rate of cumulative energy consumption and longitudinal reinforcement ratio, axial compression ratio, and shear-span ratio remained unclear. However, a more apparent linear relationship was observed with the transverse reinforcement ratio. By conducting a quantitative analysis of the transverse reinforcement ratio, the researchers proposed an modified estimation model of energy consumption capacity for reinforced concrete components with axial force. Nonetheless, the accuracy of the modified estimation model was found to be high within the range of 0–250,000 kN mm of cumulative energy consumption. For cumulative energy consumption exceeding 250,000 kN mm, further experimental and theoretical research is still required to enhance the reliability of the modified estimation model.

1. Introduction

The traditional capacity-based seismic design method is widely used due to its simplicity and practicality. However, a major drawback of this method is that it does not accurately represent the actual response of structures under earthquake forces [1]. In contrast, the energy-based design method offers a more comprehensive understanding of the effects of seismic motion characteristics, such as amplitude, spectral characteristics, and strong-motion duration, on structures. The energy-based design method considers various forms of energy input into the structure during an earthquake, including elastic strain energy, kinetic energy, damping energy consumption, and hysteresis energy consumption, all of which contribute to the structural damage [2–4]. To prevent severe damage, the seismic input energy should be kept below the total energy consumption capacity of the structure [5]. During an earthquake, the structural energy primarily dissipates through damping energy consumption and hysteresis energy consumption, as the kinetic energy and elastic strain energy can mutually convert without energy loss. However, practical engineering observations indicate that damping energy consumption only accounts for a small portion of the total energy consumption. The hysteresis energy consumption becomes the dominant factor affecting structural damage [6–8]. Therefore, the ability to accurately predict the energy consumption

capacity of structures under earthquake forces is crucial for the implementation of energy-based seismic design.

The concept and design principles of the energy-based design method were initially introduced by Housner [9]. Park and Ang [10] conducted extensive research on the damage mechanisms of reinforced concrete components under earthquake forces [10]. They proposed a two-parameter damage model that incorporates maximum deformation and cumulative energy consumption terms, which has been adopted to guide energy-based design method [11]. However, this damage model only relies on the combined parameter β to account for the complex coupling relationship between the maximum deformation term and the cumulative energy dissipation term. Moreover, the acquisition of the combined parameter β only considers the failure state of the reinforced concrete components. Therefore, while this model can effectively define the failure state, more experiments and theoretical research are still needed for the repairable state [12, 13]. Additionally, this damage model does not provide a method for determining the energy consumption capacity. Erberik and Sucuoğlu[14] conducted low-cycle reciprocating hysteresis tests on 17-reinforced concrete beam components and established a correlation between the damage mechanism of energy consumption capacity under constant and variable amplitude conditions [14, 15]. They proposed a method for determining the energy consumption capacity of reinforced concrete beam components under variable amplitude hysteresis. However, their study primarily focused on reinforced concrete beam components with plain circular steel bars as longitudinal reinforcement, limiting the applicability of their conclusions. Poljansek et al. [16] conducted a study to explore the relationship between the energy consumption capacity and residual deformation capacity of reinforced concrete column components. However, their study did not consider the effects of different loading histories. The research group conducted steady-state amplitude and arbitrary amplitude loading tests on 24-reinforced concrete components without axial force [17, 18]. The influence of loading displacement history, transverse reinforcement ratio, and longitudinal reinforcement ratio on the degradation mechanism of reinforced concrete components was analyzed, and the estimation model of energy consumption capacity for reinforced concrete components without axial force was proposed.

This study applies the estimation model of energy consumption capacity for reinforced concrete components without axial force to evaluate the energy consumption capacity of 92-reinforced concrete components in the Pacific Earthquake Engineering Research Center (PEER) database, considering axial force and bending. The research investigates the impact of design parameters on the estimation results. Building upon these findings, modifications are made to the estimation model of energy consumption capacity, leading to the proposal of an estimation model specifically tailored for the reinforced concrete components with axial force.

2. The Estimation Model of Energy Consumption Capacity for Reinforced Concrete Components without Axial Force

2.1. The Estimation Model of Energy Consumption Capacity. The influence mechanism of deformation history, cumulative energy consumption, and design parameters on the decay law of energy consumption capacity for reinforced concrete components was discussed, and the estimation model of the energy consumption capacity for reinforced concrete components without axial force was established [17].

$$E_k = 2(1 - D_k)(\mu_k - 1)M_y\theta_y, \tag{1}$$

where E_k represents the energy consumption capacity of the k-th semi-hysteresis loop. μ_k represents the nominal ductility coefficient. M_y represents the yield bending moment of the reinforced concrete components. θ_y represents the yield displacement angle of the the reinforced concrete components. D_k represents the decay index of energy consumption capacity, which can be obtained from Formula (2), when $k = 1$, the decay index of energy consumption capacity D_k is 0.

$$D_k = \begin{cases} \alpha(1 - e^{-\beta n_k})\text{IDS} \\ \alpha\left(1 - e^{-\beta(n_k - 0.54n_b)}\right)\text{SLDS} \\ \alpha(1 - e^{-\beta n_k}) + 0.002n_b\text{SSDS} \end{cases}. \tag{2}$$

Here, IDS represents the initial displacement stage, SLDS represents the subsequent large displacement stage (when the displacement deformation is greater than the historical displacement deformation, the current stage is the subsequent large displacement stage), SSDS represents the subsequent small displacement stage (when the displacement deformation is less than the historical displacement deformation, the current stage is the subsequent small displacement stage). The parameters α and β are obtained from Formulas (3) and (4), respectively. n_k is the nominal cumulative energy consumption of the k-th semi-hysteresis loop, obtained from Formula (5), and n_b is the nominal cumulative energy consumption at the subsequent displacement stage.

$$\alpha = 0.62\mu_k^{0.2}, \tag{3}$$

$$\beta = \frac{4.25\rho_t^{-0.11}}{(1 + \mu_k)^{5.28\rho_t^{0.09}}}, \tag{4}$$

where ρ_t represents the transverse reinforcement ratio of the plastic hinge area.

$$n_k = \frac{\int E_k}{0.5M_y\theta_y}, \tag{5}$$

where $\int E_k$ represents the cumulative energy consumption.

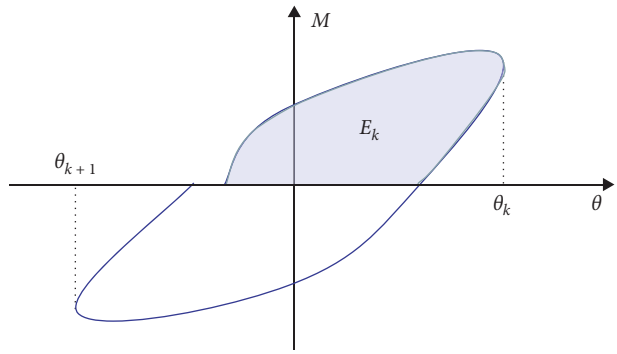

Figure 1: The energy consumption capacity of the k-th semi-hysteresis loop.

Table 1: The design parameters of 24-reinforced concrete components without axial force.

No.	ρ_t (%)	ρ (%)	N	λ	No.	ρ_t (%)	ρ (%)	N	λ
M1	0.226	0.766	0	4.28	M13	0.402	0.971	0	4.28
M2	0.226	0.766	0	4.28	M14	0.402	0.971	0	4.28
M3	0.226	0.766	0	4.28	M15	0.402	0.971	0	4.28
M4	0.402	0.766	0	4.28	M16	0.402	1.198	0	4.28
M5	0.402	0.766	0	4.28	M17	0.402	1.198	0	4.28
M6	0.402	0.766	0	4.28	M18	0.402	1.198	0	4.28
M7	0.804	0.766	0	4.28	M19	0.226	0.766	0	4.28
M8	0.804	0.766	0	4.28	M20	0.402	0.766	0	4.28
M9	0.804	0.766	0	4.28	M21	0.402	1.198	0	4.28
M10	0.402	0.587	0	4.28	M22	0.804	1.198	0	4.28
M11	0.402	0.587	0	4.28	M23	0.226	1.198	0	4.28
M12	0.402	0.587	0	4.28	M24	0.226	0.587	0	4.28

2.2. Estimation Results of Cumulative Energy Consumption. As shown in Figure 1, the shaded area represents the energy consumption capacity of the k-th semi-hysteresis loop E_k. The cumulative energy consumption is defined as the sum of the energy consumption capacities of all semi-hysteresis loops.

The cumulative energy consumption of 24-reinforced concrete components without axial force from the study of Liu et al. [17] was estimated using Formulas (1)–(5). Table 1 presents the design parameters of 24-reinforced concrete components without axial force, where ρ_t represents transverse reinforcement ratio, ρ represents longitudinal reinforcement ratio, N represents axial compression ratio, and λ represents shear-span ratio, the mention of shear-span ratio is the ratio between the shear span of the reinforced concrete component and the effective height of its cross-section.

Figure 2 shows the experimental values and estimated values of cumulative energy consumption for 24-reinforced concrete components without axial force. The horizontal axis is the experimental values of cumulative energy consumption, while the vertical axis is the estimated values of cumulative energy consumption. The red solid line represents the $y = x$ line, and the data points located on this red solid line indicate that the experimental value is equal to the estimated value. The green solid line represents the ±20% error line. From the Figure 2, it can be observed that the data points are distributed around the red solid line, indicating a generally good agreement between the experimental and estimated

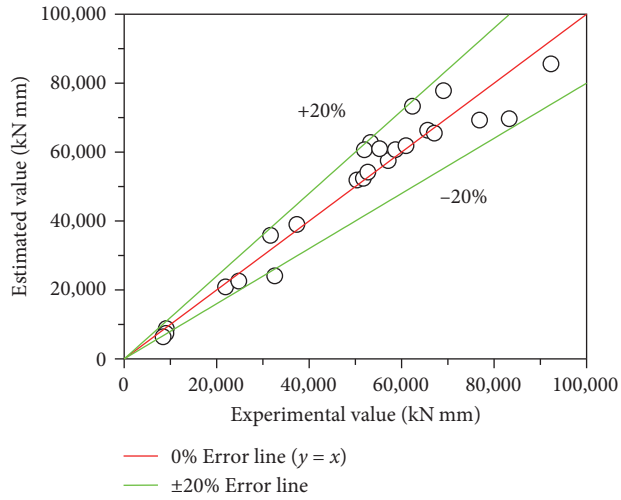

Figure 2: Experimental values and estimated values of cumulative energy consumption for 24-reinforced concrete components without axial force.

Table 2: The design parameters of 92-reinforced concrete components with axial force.

No.	ID	ρ_t (%)	ρ (%)	N	λ	No.	ID	ρ_t (%)	ρ (%)	N	λ
P1	Gill et al. No. 3	0.762	0.895	0.42	2.18	P47	Sakai et al. B5	0.848	1.605	0.131	2.86
P2	Gill et al. No. 4	1.327	0.895	0.6	2.18	P48	Sakai et al. B6	0.848	1.605	0.126	2.86
P3	Ang et al.No. 3	1.131	0.755	0.1	4	P49	Atalay et al. No. 4S1	1.573	1.775	0.2	2
P4	Ang et al. No. 4	0.873	0.755	0.21	4	P50	Atalay et al. No. 5S1	0.807	0.93	0.599	2
P5	Soesianawati et al. No. 2	0.644	0.755	0.3	4	P51	Atalay et al. No. 6S1	1.271	0.93	0.599	2
P6	Soesianawati et al. No. 3	0.423	0.755	0.3	4	P52	Atalay et al. No. 9	1.634	0.93	0.599	2
P7	Soesianawati et al. No. 4	0.301	0.755	0.3	4	P53	Atalay et al. No. 10	0.098	0.505	0.339	7.64
P8	Zahn et al. No. 7	0.671	0.755	0.223	4	P54	Atalay et al. No. 12	1.388	1.29	0.5	6.04
P9	Zahn et al. No. 8	0.854	0.755	0.39	4	P55	Azizinamini et al. NC-4	1.242	1.29	0.36	6.04
P10	Watson et al. No. 5	0.621	0.755	0.5	4	P56	Saatcioglu et al. U3	1.242	1.29	0.5	6.04
P11	Watson et al. No. 6	0.295	0.755	0.5	4	P57	Saatcioglu et al. U6	2.49	1.29	0.45	6.04
P12	Watson et al. No. 8	0.653	0.755	0.7	4	P58	Saatcioglu et al. U7	1.883	1.29	0.47	6.04
P13	Tanaka et al. No. 1	1.06	0.785	0.2	4	P59	Xiao et al. 0.2P	0.4	0.975	0.428	4.7
P14	Tanaka et al. No. 2	1.06	0.785	0.2	4	P60	Sugano UC10H	0.799	0.975	0.428	4.7
P15	Tanaka et al. No. 3	1.06	0.785	0.2	4	P61	Sugano UC15H	0.533	1.465	0.462	4.7
P16	Tanaka et al. No. 4	1.06	0.785	0.2	4	P62	Sugano UC20H	1.066	1.465	0.462	4.7
P17	Tanaka et al. No. 5	0.748	0.625	0.1	3	P63	Nosho et al. No. 1	1.066	1.145	0.456	4.7
P18	Tanaka et al. No. 6	0.748	0.625	0.1	3	P64	Bayrak et al. ES-1HT	0.514	1.465	0.462	4.7
P19	Tanaka et al. No. 7	0.914	0.625	0.3	3	P65	Bayrak et al. AS-2HT	0.514	1.465	0.231	4.7
P20	Tanaka et al.No. 8	0.914	0.625	0.3	3	P66	Bayrak et al. AS-3HT	0.514	1.64	0.462	4.7
P21	Park et al. No. 9	1.06	0.94	0.1	2.97	P67	Bayrak et al. AS-5HT	1.066	1.64	0.462	4.7
P22	Zhou et al. No. 214-08	0.614	1.11	0.8	2	P68	Bayrak et al. ES-8HT	0.916	0.965	0.102	3
P23	Kanda et al. 85STC-1	0.38	0.81	0.106	3	P69	Saatcioglu et al. BG-1	0.905	0.965	0.102	3
P24	Kanda et al. 85STC-2	0.38	0.81	0.106	3	P70	Saatcioglu et al. BG-2	0.916	0.965	0.211	3
P25	Kanda et al. 85STC-3	0.38	0.81	0.106	3	P71	Saatcioglu et al. BG-4	0.905	0.965	0.211	3
P26	Kanda et al. 85PDC-1	0.38	0.81	0.119	3	P72	Saatcioglu et al. BG-5	0.916	0.965	0.143	3
P27	Muguruma et al. AL-1	1.616	1.9	0.4	2.5	P73	Saatcioglu et al. BG-6	0.905	0.965	0.143	3
P28	Muguruma et al. AH-1	1.616	1.9	0.4	2.5	P74	Saatcioglu et al. BG-7	0.623	1.07	0.113	3.5
P29	Muguruma et al. AL-2	1.616	1.9	0.629	2.5	P75	Saatcioglu et al. BG-8	0.623	1.07	0.158	3.5
P30	Mugumura et al. AH-2	1.616	1.9	0.629	2.5	P76	Saatcioglu et al. BG-9	0.623	1.07	0.216	3.5
P31	Muguruma et al. BH-1	1.616	1.9	0.254	2.5	P77	Saatcioglu et al. BG-10	0.599	1.07	0.111	3.5
P32	Muguruma et al. BL-2	1.616	1.9	0.423	2.5	P78	Matamoros et al. C10-10N	0.599	1.07	0.156	3.5
P33	Muguruma et al. BH-2	1.616	1.9	0.423	2.5	P79	Matamoros et al. C10-10S	0.599	1.07	0.21	3.5
P34	Sakai et al. B1	0.524	1.215	0.35	2	P80	Matamoros et al. C10-20N	0.577	1.07	0.107	3.5
P35	Sakai et al. B2	0.785	1.215	0.35	2	P81	Matamoros et al. C10-20S	0.577	1.07	0.154	3.5
P36	Sakai et al. B4	0.524	1.215	0.35	2	P82	Matamoros et al. C5-20N	0.623	1.225	0.2	3.92
P37	Sakai et al. B5	0.524%	1.215	0.35	2	P83	Matamoros et al. C5-20S	0.706	1.225	0.1	3.92
P38	Sakai et al. B6	0.513	1.215	0.35	2	P84	Mo et al. C1-1	0.706	1.225	0.2	3.92
P39	Atalay et al. No. 4S1	0.366%	0.815	0.104	5.5	P85	Mo et al. C1-2	0.564	1.225	0.2	3.92
P40	Atalay et al. No. 5S1	0.612	0.815%	0.195	5.5	P86	Mo et al.C1-3	0.471	1.225	0.2	3.92
P41	Atalay et al. No. 6S1	0.366	0.815	0.181	5.5	P87	Mo et al. C2-1	0.403	1.225	0.2	3.92
P42	Atalay et al. No.9	0.612	0.815%	0.259	5.5	P88	Mo et al.C2-2	1.863	1.075	0.14	6.56
P43	Atalay et al.No. 10	0.366	0.815	0.266	5.5	P89	Mo et al. C2-3	1.863	1.075	0.277	6.56
P44	Atalay et al. No. 12	0.366	0.815	0.271	5.5	P90	Mo et al. C3-1	0.86	1.075	0.136	6.56
P45	Azizinamini et al. NC-4	0.517	0.97	0.31	3	P91	Mo et al. C3-2	2.033	1.075	0.53	6.56
P46	Saatcioglu et al. U3	0.598	1.605	0.141	2.86	P92	Thomsen et al. A3	1.863	1.075	0.506	6.56

values. The maximum absolute error between the two sets of values is within 20%, which suggests that the estimation model proposed in [17] exhibits high accuracy in estimating the cumulative energy consumption of reinforced concrete components without axial force.

In order to verify the applicability of the estimation model for reinforced concrete components with axial force, the original data of 92-reinforced concrete components were extracted from the PEER database based on the following criteria: (1) presence of axial force, (2) rectangular cross-

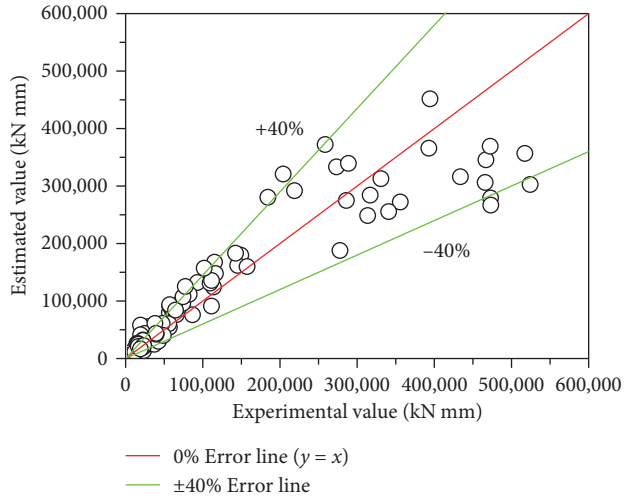

Figure 3: Experimental values and estimated values of cumulative energy consumption for 92-reinforced concrete components with axial force.

section, and (3) bending failure as the failure mode. The design parameters for 92-reinforced concrete components with axial force are shown in Table 2.

Figure 3 shows the experimental values and estimated values of cumulative energy consumption for 92-reinforced concrete components with axial force. The horizontal axis is the experimental values of cumulative energy consumption, and the vertical axis is the estimated values of cumulative energy consumption. The red solid line represents the $y = x$ line, the green solid line represents the $\pm 40\%$ error line. It can be seen from the Figure 3 that the data points are distributed around the red solid line but with significant dispersion. The maximum absolute error is around 40%. This indicates that when using the estimation model of energy consumption capacity for reinforced concrete components without axial force to calculate the energy consumption capacity of 92-reinforced concrete components subjected to axial force and bending, the estimation error of cumulative energy consumption is relatively large.

3. The Modified Estimation Model of Energy Consumption Capacity for Reinforced Concrete Components with Axial Forces

3.1. Estimation Error Rate of Cumulative Energy Consumption. In order to describe the accuracy of the estimation model for energy consumption capacity, the estimation error rate ε of cumulative energy consumption is defined as follows:

$$\varepsilon = \left(\frac{\int E_{ex}}{\int E_{es}} - 1 \right) \times 100\%, \tag{6}$$

where $\int E_{ex}$ is the experimental value of cumulative energy consumption and $\int E_{es}$ is the estimated value of cumulative energy consumption.

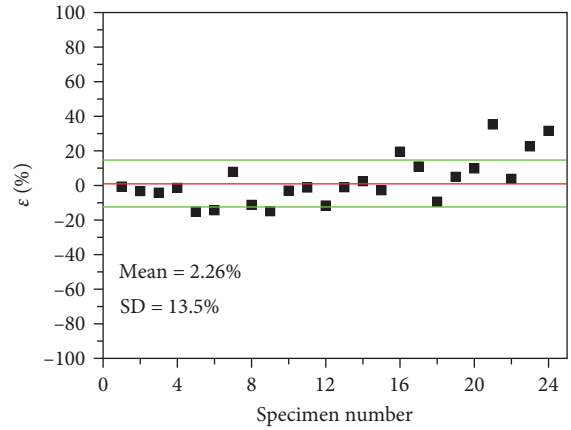

Figure 4: The estimation error rate ε of cumulative energy consumption for 24-reinforced concrete components without axial force.

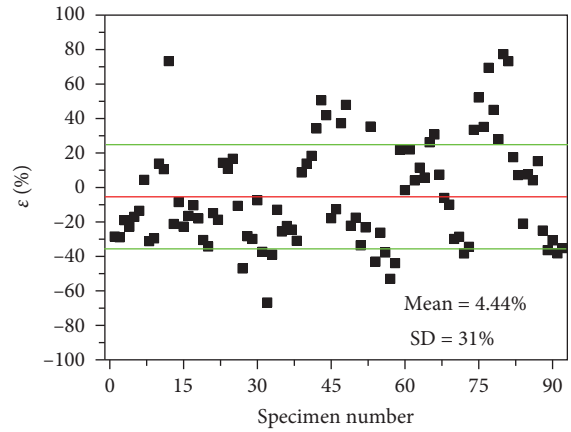

Figure 5: The estimation error rate ε of cumulative energy consumption for 92-reinforced concrete components with axial force.

Figures 4 and 5 show the estimation error rate ε of cumulative energy consumption for 24-reinforced concrete components without axial force and 92-reinforced concrete components with axial force, respectively. In the Figures 4 and 5, the horizontal axis is the specimen number, and the vertical axis is the estimation error rate ε of cumulative energy consumption. The red solid line represents the mean value of estimation error rate, and the green solid line represents ± 1 standard deviation.

As shown in Figure 4, the mean value of estimation error rate ε and standard deviation of cumulative energy consumption for reinforced concrete components without axial force are 2.26% and 13.5%, respectively. This indicates that the proposed estimation model has a high accuracy in estimating the cumulative energy consumption of reinforced concrete components without axial force. As shown in Figure 5, the mean value of estimation error rate ε and standard deviation of cumulative energy consumption for reinforced concrete components with axial force are 4.44% and 31%, respectively. Comparing Figures 4 and 5, it can be observed that when using the estimation model to estimate

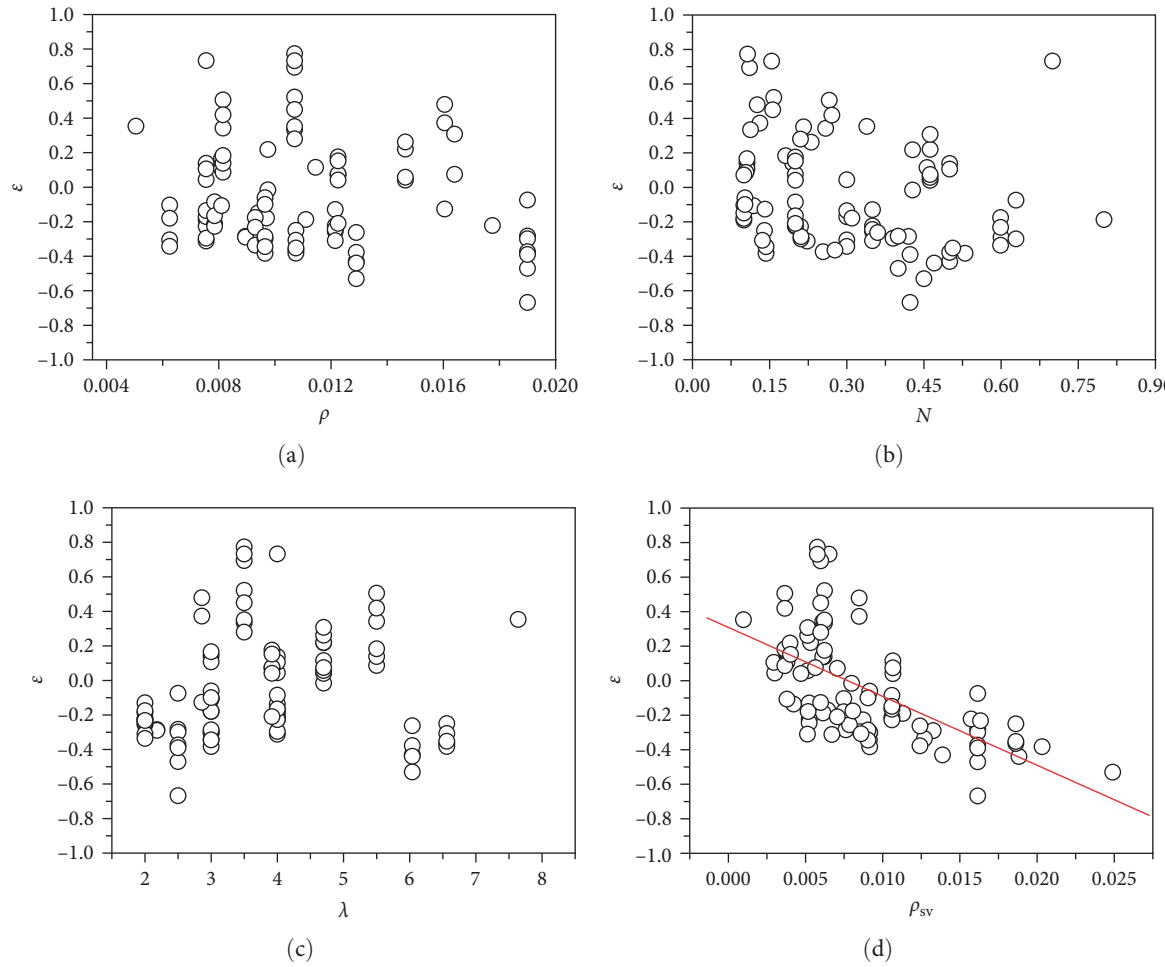

FIGURE 6: The correlation between design parameters and estimation error rate ε. (a) The correlation between longitudinal reinforcement ratio ρ and estimation error rate ε. (b) The correlation between axial compression ratio N and estimation error rate ε. (c) The correlation between shear-span ratio λ andestimation error rate ε. (d) The correlation between transverse reinforcement ratio ρ_t and estimation error rate ε.

the reinforced concrete components with axial force, both the accuracy and stability of the estimation model are not ideal. In order to analyze the influencing factors that cause the above results, the correlation between design parameters (longitudinal reinforcement ratio ρ, transverse reinforcement ratio ρ_t, axial compression ratio N, and shear-span ratio λ) and the estimation error rate ε of cumulative energy consumption is preliminarily analyzed.

Figure 6(a) shows the correlation between longitudinal reinforcement ratio ρ and estimation error rate ε, where the variation range of longitudinal reinforcement ratio ρ is 0.625%–o1.775%. Figure 6(b) shows the correlation between the axial compression ratio N and estimation error rate ε, where the variation range of the axial compression ratio N is 0.1–0.8. Figure 6(c) shows the correlation between the shear-span ratio λ and estimation error rate ε, where the variation range of the shear-span ratio λ is 2–7.64. Overall, the data points in Figure 6(a)–6(c), exhibit significant dispersion, indicating that there is a lack of sufficient correlation between the longitudinal reinforcement ratio ρ, axial compression ratio N, shear-span ratio λ, and the estimated error rate ε of cumulative energy consumption.

Figure 6(d) shows the correlation between transverse reinforcement ratio ρ_t and estimation error rate ε, where the variation range of transverse reinforcement ratio ρ_t is 0.098%–1.863%. From Figure 6(d), it can be observed that there is a certain linear relationship between the transverse reinforcement ratio ρ_t and the estimation error rate ε of cumulative energy consumption. As the transverse reinforcement ratio ρ_t increases, the estimation error rate ε gradually decreases. Therefore, the modification of the estimation model will focus on the transverse reinforcement ratio ρ_t.

3.2. The Modified Estimation Model of the Energy Consumption Capacity. According to the estimation model of energy consumption capacity for reinforced concrete components without axial force, only Formula (4) contains the transverse reinforcement ratio ρ_t in the entire estimation process. Therefore, the modification of the estimation model of the energy consumption capacity focuses on parameter β. Previous research has found that by modifying the magnitude of the transverse reinforcement ratio ρ_t, it is possible to effectively change the estimated value of cumulative energy consumption and continuously reduce the estimation error

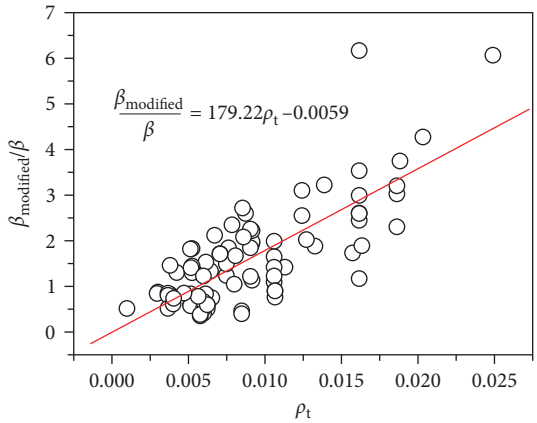

FIGURE 7: The relationship between parameter β, modified parameter $\beta_{modified}$ and the transverse reinforcement ratio ρ_t.

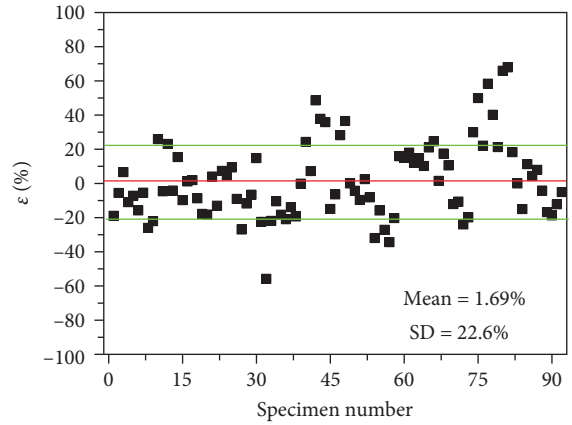

FIGURE 8: The estimation error rate of cumulative energy consumption for 92-reinforced concrete components with axial force calculated by the modified estimation model.

rate ε of energy consumption capacity to an ideal state [17]. Therefore, in order to achieve an estimation error rate ε of energy consumption capacity within $\pm 5\%$ and determine the modified transverse reinforcement ratio $\rho_{t,modified}$, regression equations are used [18].

By substituting the modified transverse reinforcement ratio $\rho_{t,modified}$ into Formula (4), the modified parameter $\beta_{modified}$ can be obtained. To further explore the relationship between parameter β, modified parameter $\beta_{modified}$, and the transverse reinforcement ratio ρ_t, the data of the three variables are summarized in Figure 7. The vertical axis is the ratio of the modified parameter $\beta_{modified}$ to the parameter β, and the horizontal axis is the transverse reinforcement ratio ρ_t.

As shown in Figure 7, the ratio of the modified parameter $\beta_{modified}$ to the parameter β increases linearly with the increase of the transverse reinforcement ratio ρ_t. By linearly fitting the data points in Figure 7, the Formula (7) can be obtained as follows:

$$\frac{\beta_{modified}}{\beta} = 179.22\rho_t - 0.0059. \tag{7}$$

Bring Formula (7) into Formula (4), the modified parameter $\beta_{modified}$ can be obtained as follows:

$$\beta_{modified} = \frac{4.25\rho_t^{-0.11}}{(1+\mu_k)^{5.28\rho_t^{0.09}}}(179.22\rho_t - 0.0059). \tag{8}$$

By replacing the Formula (4) with Formula (8), the modified estimation model of energy consumption capacity for reinforced concrete components with axial forces can be obtained.

4. Evaluation of Modified Estimation Model

Figure 8 shows the estimated error rate ε of cumulative energy consumption for 92-reinforced concrete components with axial force calculated by the modified estimation model. In the Figure 8, the horizontal axis is the specimen number and the vertical axis is the estimation error rate ε of cumulative energy consumption. The red solid line represents the mean value of estimation error rate, and the green solid line represents plus or minus one standard deviation.

As shown in Figure 8, the mean value and standard deviation of the estimation error rate ε calculated by the modified estimation model are 1.69% and 22.6%, respectively. By comparing Figure 8 with Figure 5, it can be observed that the mean value of estimation error rate ε is reduced by 2.75% compared to the original estimation model, and the standard deviation of estimation error rate ε is reduced by 8.4% compared to the original estimation model. This indicates that the accuracy and stability of the modified estimation model have been improved when estimating the reinforced concrete components with axial force.

To describe the accuracy of the modified estimation model, the Pearson correlation coefficient r is used to evaluate the experimental value and estimated value, the closer the Pearson correlation coefficient r is to 1, the closer the estimated value is to the experimental value. The Pearson correlation coefficient r is defined as follows:

$$r = \frac{\sum(X-\overline{X})(Y-\overline{Y})}{\sqrt{\sum(X-\overline{X})^2\sum(Y-\overline{Y})^2}}, \tag{9}$$

where X and Y represent the values of two variables. When $0.8 < r \leq 1.0$, it indicates a very high correlation, when $0.7 < r \leq 0.8$, it indicates a high correlation; when $0.4 < r \leq 0.7$, it indicates a moderate correlation; when $0.2 < r \leq 0.4$, it indicates a low correlation; when $0 < r \leq 0.2$, it indicates no correlation.

Figure 9(a) shows the experimental values and estimated values calculated by the original estimation model for 92-reinforced concrete components with axial force, and Pearson correlation coefficient r is 0.921. Figure 9(b) shows the experimental values and estimated values calculated by the modified estimation model for 92-reinforced concrete

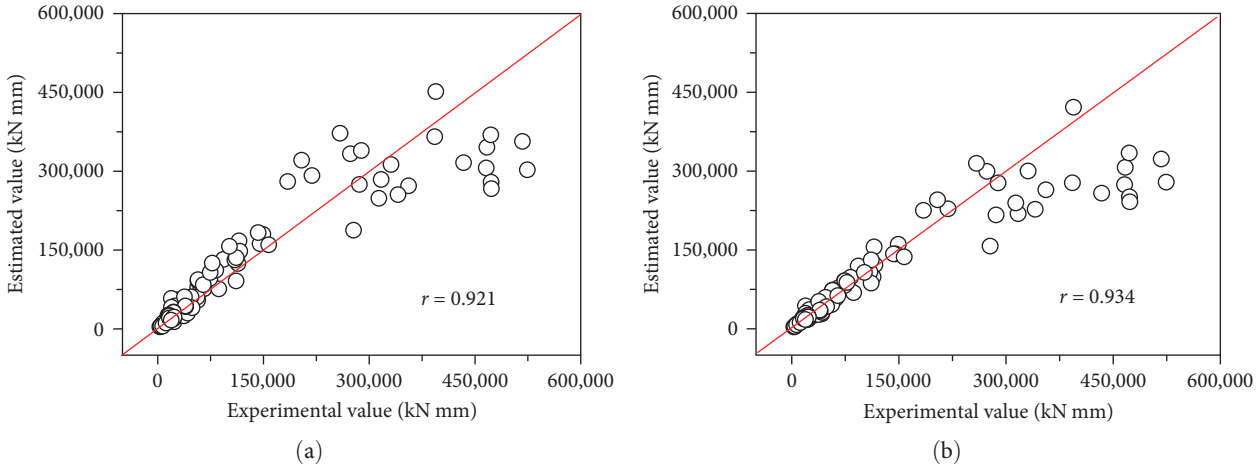

Figure 9: The experimental values and estimated values. (a) The experimental values and estimated values calculated by the original estimation model. (b) The experimental values and estimated values calculated by the modified estimation model.

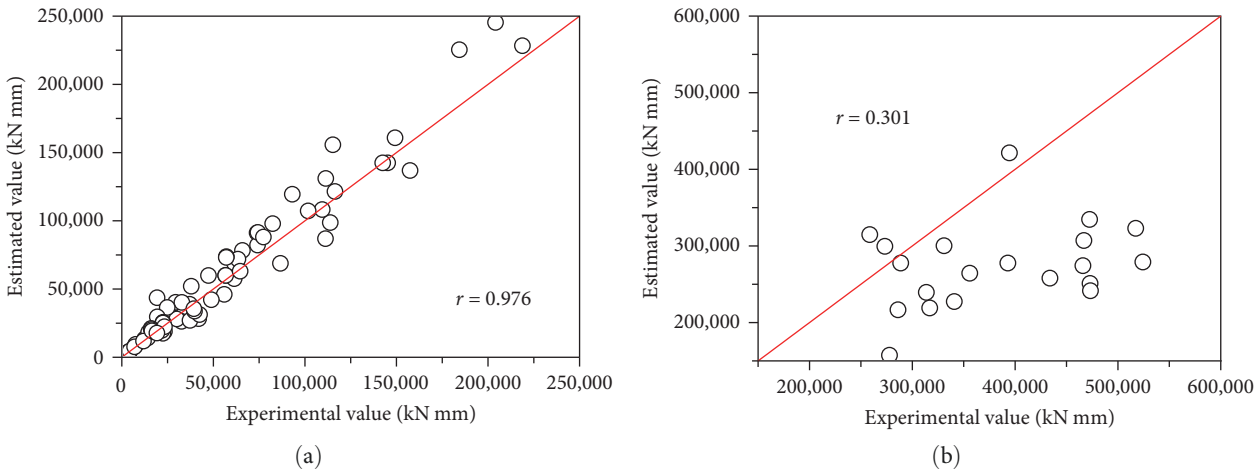

Figure 10: The experimental values and estimated values calculated by the modified estimation model. (a) The experimental values and estimated values calculated by the modified estimation model of cumulative energy consumption in the range of 0–250,000 kN mm. (b) The experimental values and estimated values calculated by the modified estimation model of cumulative energy consumption in the range of 250,000–600,000 kN mm.

components with axial force, and Pearson correlation coefficient r is 0.934. It can be seen that the estimated values calculated by the modified estimation model are closer to the experimental values.

Figure 10(a) shows the experimental values and estimated values calculated by the modified estimation model of cumulative energy consumption in the range of 0–250,000 kN mm, and Pearson correlation coefficient r is 0.976. Figure 10(b) shows the experimental values and estimated values calculated by the modified estimation model of cumulative energy consumption in the range of 250,000–600,000 kN mm, and Pearson correlation coefficient r is only 0.301. It can be seen that the modified estimation model has high accuracy in estimating cumulative energy consumption in the range of 0–250,000 kN mm. When the cumulative energy consumption exceeds 250,000 kN mm, the accuracy of the modified estimation model in estimating cumulative energy consumption is relatively low. This phenomenon may be related to the cumulative energy consumption of the designed specimens in [17] (the cumulative energy consumption is in the range of 0–100,000 kN mm).

5. Conclusions

To study energy-based seismic design methods, it is necessary to accurately predict the energy consumption capacity of reinforced concrete members under earthquake forces. In this paper, the estimation model of energy consumption capacity for reinforced concrete components with axial force is proposed by modifying the estimation model of energy consumption capacity for reinforced concrete components without axial force. Based on the results of this study, the following conclusions have been reached:

(1) When using the estimation model of energy consumption capacity for reinforced concrete components

without axial force to calculate the energy consumption capacity of reinforced concrete components with axial force, the estimation deviation rate of cumulative energy consumption is relatively large.

(2) The modified estimation model for predicting the energy consumption capacity of reinforced concrete components with axial force is proposed, and the accuracy of the modified estimation model is high when the cumulative energy consumption is in the range of 0–250,000 kN mm.

(3) To enhance the applicability of the proposed estimation method, effective and sufficient experiments should be conducted to refine the proposed estimation model when the energy dissipation capacity exceeds 250,000 kN mm.

Data Availability

The data used to support the findings of this study are available from the corresponding author upon request.

Conflicts of Interest

The authors declare that they have no conflicts of interest.

Acknowledgments

This research was supported by the Natural Science Foundation of Hunan Province (Grant No. 2022JJ40023), the Scientific Research Project of Education Department of Hunan Province (Grant No. 20B108), the Yiyang City Science and Technology Special Funds Project (Grant No. 2021133), the Aid Program for Science and Technology Innovative Research Team in Higher Educational Institutions of Hunan Province.

References

[1] M. J. N. Priestley, "Performance based seismic design," *Bulletin of the New Zealand Society for Earthquake Engineering*, vol. 33, no. 3, pp. 325–346, 2000.

[2] H. Li and X.-G. Ye, "Research on the elastic–plastic input energy spectra based on compound intensity indicator," *Engineering Mechanics*, vol. 30, no. 4, pp. 7–14, 2013.

[3] C. Qiu, J. Qi, and C. Chen, "Energy-based seismic design methodology of SMABFs using hysteretic energy spectrum," *Journal of Structural Engineering*, vol. 146, no. 2, Article ID 04019207, 2020.

[4] L. Ye, G. Cheng, Z. Qu, and X. Lu, "Study on energy-based seismic design method and application on steel braced frame structures," *Journal of Building Structures*, vol. 33, no. 11, pp. 36–45, 2012.

[5] C.-C. Chou and C.-M. Uang, "A procedure for evaluating seismic energy demand of framed structures," *Earthquake Engineering Structural Dynamics*, vol. 32, no. 2, pp. 229–244, 2003.

[6] Y.-K. Wang, Z.-F. Liu, D. Zhang, and Z.-Q. Hu, "Research on energy based seismic design method of RC beam members," *Engineering Mechanics*, vol. 40, no. 11, pp. 1–9, 2023.

[7] G. Song, T. Y. Yang, and Y. Zhou, "Energy-based seismic design for self-centering concrete frames," *Bulletin of Earthquake Engineering*, vol. 19, pp. 5113–5137, 2021.

[8] N. Gholami, S. Garivani, S. S. Askariani, and I. Hajirasouliha, "Estimation of hysteretic energy distribution for energy-based design of structures equipped with dampers," *Journal of Building Engineering*, vol. 51, Article ID 104221, 2022.

[9] G. W. Housner, "Limit design of structures to resist earthquakes," in *Proceedings of the First World Conference on Earthquake Engineering*, pp. 1–12, Earthquake Engineering Research Institute, Berkeley, California, 1956.

[10] Y.-J. Park and A. H.-S. Ang, "Mechanistic seismic damage model for reinforced concrete," *Journal of Structural Engineering*, vol. 111, no. 4, pp. 722–739, 1985.

[11] Y.-J. Park, A. H.-S. Ang, and Y. K. Wen, "Seismic damage analysis of reinforced concrete buildings," *Journal of Structural Engineering*, vol. 111, no. 4, 1985.

[12] Z. Liu, H. Yuan, and M. Duan, "Experimental study of plastic energy dissipation capacity deterioration of RC beams under variable amplitude loading histories," *Journal of Building Structures*, vol. 36, no. 4, pp. 75–85, 2015.

[13] Z. Liu, Y. Wang, H. Yuan, and K. Chen, "Damage evaluation of RC beams under variable amplitude loading histories," *Journal of Building Structures*, vol. 38, no. 11, pp. 132–141, 2017.

[14] A. Erberik and H. Sucuoğlu, "Seismic energy dissipation in deteriorating systems through low-cycle fatigue," *Earthquake Engineering Structural Dynamics*, vol. 33, no. 1, pp. 49–67, 2004.

[15] H. Sucuoğlu and A. Erberik, "Energy-based hysteresis and damage models for deteriorating systems," *Earthquake Engineering Structural Dynamics*, vol. 33, no. 1, pp. 69–88, 2004.

[16] K. Poljansek, I. Perus, and P. Fajfar, "Hysteretic energy dissipation capacity and the cyclic to monotonic drift ratio for rectangular RC columns in flexure," *Earthquake Engineering Structural Dynamics*, vol. 38, no. 7, pp. 907–928, 2009.

[17] Z. Liu, Y. Wang, Z. Cao, Y. Chen, and Y. Hu, "Seismic energy dissipation under variable amplitude loading for rectangular RC members in flexure," *Earthquake Engineering Structural Dynamics*, vol. 47, no. 4, pp. 831–853, 2018.

[18] Y. Wang, Z. Liu, W. Yang, Y. Hu, and Y. Chen, "Damage index of reinforced concrete members based on the energy dissipation capability degradation," *The Structural Design of Tall and Special Buildings*, vol. 29, no. 2, Article ID e1695, 2020.